Synthesis and structural characterization of dry $AgPO_3$ glass by Raman scattering, infrared reflectance, and modulated differential scanning calorimetry

Deassy I. Novita and P. Boolchand
Department of Electrical and Computer Engineering, University of Cincinnati, Cincinnati, Ohio 45221-0030, USA
(Received 13 April 2007; revised manuscript received 20 August 2007; published 28 November 2007)

The glass transition temperatures of $AgPO_3$ have been reported to lie in the $163 < T_g < 192$ °C range. These results are typical when precursors are processed at laboratory ambient. In the present work, we show that if precursors are handled in a dry ambient environment, the T_g's steadily increase in the $181(2) < T_g < 254(2)$ °C range as the relative humidity of the ambient environment decreases. The glass transition temperature of dry $AgPO_3$ is found to be 254(2) °C. We have compared the vibrational densities of states of the low-T_g [181(2) °C] and high-T_g [254(2) °C] samples in Raman scattering and ir reflectance measurements. The ir reflectance shows the presence of both free and bonded water in the low-T_g [181(2) °C] samples, but the concentration of both species decreases in the high-T_g [254(2) °C] samples. In Raman scattering, the boson peak scattering strength increases, and the scattering strength ratio R of the P-O_t (terminal) to the P-O_b (bridging) mode of the P-O-P- chains decreases as the sample T_g increases. The presence of bonded water serves to scission the P-O-P chain network by replacing bridging O_b oxygen sites with terminal OH^- species; and once incorporated, bonded water is difficult to remove.

DOI: 10.1103/PhysRevB.76.184205 PACS number(s): 61.43.Fs, 63.50.+x, 78.30.Ly

I. INTRODUCTION

The influence of water on the physical behavior of network glasses is a problem of interest both in basic science and applications of these materials. Naraev[1] in a recent review has highlighted the influence of structurally bonded water (OH groups) on the electrical behavior of sodium silicate glasses. Takata *et al.*[2] found the electrical conductivity of modified oxide glasses to display in many cases a global minimum near a few weight percent of H_2O; a behavior quite similar to that of Na_2O as an additive in silicate glasses. The origin of such a threshold behavior remains largely an open issue. Recently, Rompicharla *et al.*[3] have observed that the glass transitions of dry $(Na_2O)_x(GeO_2)_{1-x}$ glasses are generally hysteretic at $x < 14\%$ and at $x > 19\%$, but these become nonhysteretic or thermally reversible in the $14\% < x < 19\%$ range (the reversibility window). The reversibility window is readily observed in dry samples[4,5] but it nearly collapses in wet ones.[3,5] Reversibility windows are observed[6] in chalcogenide glasses as well and are identified with intermediate phases. Upon alloying iodine atoms in base chalcogenide glasses, these windows are also known[7,8] to collapse. In these instances it appears that replacement of bridging O atoms by dangling OH^- groups in oxide glasses, or the replacement of bridging S or Se atoms by dangling iodine atoms in chalcogenide glasses, produces similar effects. The speculation is that dangling ends serve to cut characteristic rings where isostatic rigidity is nucleated, leading to the collapse of reversibility windows. Understanding water doping effects in oxides glasses at a basic level holds the promise of unraveling the narrowing and subsequent loss of the compositional windows across which intermediate phases form (see below).

The effect of doping water in alkali-metal–alkaline-earth-metal silicate melts has been of interest in earth sciences.[9] Water-doping-induced changes in diffusivities, redox potentials, and viscosities of silicate melts are issues that have been examined by geologists to understand magmas.[9] Water in carbohydrates has been examined in ir absorbance experiments,[10–13] and strong evidence for icelike monolayers in hygroscopic disaccharides has evolved as mid-ir bands narrow and grow in strength as water is added.

Among the oxides, phosphate glasses have enjoyed special interest because of their biocompatibility, low softening temperature, and high thermal expansion.[14] Furthermore, silver-based solid electrolytes, when used as additives in base oxide[15] and chalcogenide[16] glasses, can increase the electrical conductivities significantly. The solid electrolyte $(AgPO_3)_{1-x}(AgI)_x$ glass system has been extensively examined over the past two decades,[15,17,18] and the electrical conductivity results are notoriously nonreproducible. We have suggested[19] that the behavior may be related to the presence of water in the base $AgPO_3$ glass used in these studies. Solid electrolyte glasses have found applications in fuel cells, as sensors,[20] and as materials for flat panel displays.[21] Unfortunately, the chemical stability of some phosphate glasses is not high and this has been an impediment in their applications. Basic understanding of the issues underlying the behavior is thus of growing interest in applications of these materials.

Pseudobinary oxide glasses of the composition $(Ag_2O)_n(P_2O_5)_{1-n}$ with $n=0.5$ are generally known as metaphosphate glasses. Crystalline $AgPO_3$ has a polymorph that consists of infinitely long helical chains of PO_4 tetrahedral units[22] with four such units in a pitch. In a PO_4 unit, P has two bridging (O_b) and two nonbridging or terminal (O_t) oxygen near neighbors. Each PO_4 unit carries a negative charge and has a compensating Ag^+ cation, giving the compound $AgPO_3$ stoichiometry. Crystalline $AgPO_3$ also exists in other polymorphs that consists of trimers and tetramers, i.e., three and four $AgPO_3$ units come together to form small rings.[23] These rings are coupled to each other by weaker van der Waals forces. The structural, physical, and chemical properties of phosphate glasses has been the subject of some excellent reviews.[14,24]

In this work, we attempt to understand the affinity of $AgPO_3$ glass for water.[25,26] We have succeeded in preparing samples with a T_g of 254(2) °C. This value of T_g is significantly higher than those reported in the literature.[15,26–31] We identify the high T_g with "dry" $AgPO_3$ glass samples. We have also synthesized glass samples of lower T_g by reacting precursors at laboratory ambient (~50% relative humidity). We find that not only the magnitude of T_g but also the nature of the glass transition endotherm changes markedly when water is incorporated. To understand the structural manifestations of water doping, we have performed Raman scattering and Fourier transform ir experiments. Infrared reflectance experiments reveal the presence of both free and bonded water. In Raman scattering, the scattering strength of the Bose peak steadily increases as the T_g of the samples increases, indicating a better defined intermediate-range order in the drier samples. Furthermore, in the bond-stretching regime, the scattering strength ratio R of the Raman-active modes of P-O_t to those of P-O_b is found to steadily decrease as the T_g of the samples increases. The present results provide insights into the chemical stability of $AgPO_3$ glass, results that will also have a bearing on applications of the material.

Good glasses usually form over a very select region of phase space that is identified with intermediate phases.[32–36] Recent work,[32–36] both theoretical and experimental reveals that intermediate phases represent rigid but stress-free networks and acquire special functionalities, which are identified with self-organization of disordered networks. Dry $AgPO_3$ is a stressed rigid glass, but by alloying 10 mol % of AgI, it becomes self-organized as shown recently.[19] In this respect, good glasses can be viewed as the ultimate nanostructured functional materials.

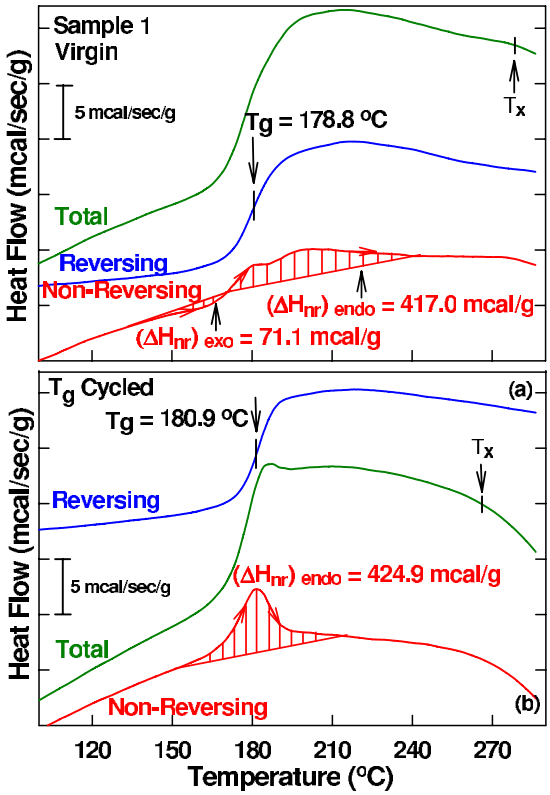

FIG. 1. (Color online) MDSC scan of sample 1 of $AgPO_3$ glass in its (a) virgin and (b) T_g-cycled state. Note that the non-reversing heat (hashed marked region) shows an exotherm prior to the glass transition endotherm in the virgin samples. The exotherm is absent in the T_g-annealed sample. T_x represents the crystallization temperature.

II. EXPERIMENT

A. Synthesis

We have synthesized four sets of $AgPO_3$ glass samples by handling the precursors in progressively drier ambient environments. Below we provide details of the synthesis.

Sample 1. Equimolar amounts of anhydrous 99.99% $AgNO_3$ powder (Fisher Scientific Inc.) and 99.999% $NH_4H_2PO_4$ powders (Alfa Aesar Inc.) were weighed and thoroughly mixed at laboratory ambient (relative humidity ~50%). All purities reflect metal content only. The mixture, contained in alumina boats, was next transferred to a box oven held at 125 °C in a chemical hood purged with laboratory air. The mixture was heated to 700 °C at a rate of 100 °C/h. Melts were held at 700 °C overnight, leading to the formation of $AgPO_3$ by the reaction

$$AgNO_3 + NH_4H_2PO_4 = AgPO_3 + H_2O + NH_4NO_3. \quad (1)$$

Melts were quenched over a pair of polished steel plates. The resulting glass samples were then stored either in a dry-nitrogen-purged glove box or encapsulated in evacuated (~10^{-7} Torr) Pyrex tubing. All glass samples were cycled through T_g to relieve stress frozen in upon quenching. The T_g of such samples is found (Fig. 1) to be 181(2) °C, typical of previous reports.[15,26–31]

Sample 2. The procedure described above for sample 1 was replicated with one change. The same starting materials this time were mixed in a nitrogen-gas-purged glove bag (relative humidity 5–10 %). The mixture was then transferred to a box furnace as described above. Such samples, henceforth labeled 2, showed a glass transition of 203(2) °C, about 20 °C higher than sample 1.

Sample 3. The procedure described above for synthesis of sample 1 was replicated with one change. Weighing and mixing of the precursors was performed in a dry-N_2-gas-purged glove box (Vacuum Atmospheres model HE-493/MO-5) with relative humidity (RH) below 0.2%. The mixture was then quickly transferred to a box oven held at 125 °C, and the precursors were reacted as described above for sample 1 or 2.

In a separate experiment, we repeated the processing described above but this time changed the precursors to 99.9% Ag_3PO_4 (Alfa Aesar Inc.) and 99.9% P_2O_5 (Fisher Scientific Inc.). The stoichiometric mixture was reacted to produce $AgPO_3$ by the reaction

$$Ag_3PO_4 + P_2O_5 = 3(AgPO_3). \quad (2)$$

The mixture was slowly heated to 900 °C (~50 °C above the melting point of Ag_3PO_4) at 100 °C/h, and the melts were held at 700 °C overnight before quenching them on

steel plates. We obtained the same T_g of 242(2) °C for $AgPO_3$ glass using either reaction (1) or reaction (2) (Fig. 2). The independence of T_g on precursors suggests that the higher T_g is intrinsic to $AgPO_3$ glass.

Sample 4. Since the precursors used in the synthesis of samples above were opened in the laboratory ambient, we decided to obtain a fresh stock of the starting materials (Ag_3PO_4 and P_2O_5) from the suppliers. The containing bottles were let stand in the purged glove box overnight before opening, weighing, and mixing the starting materials. Mixtures of the starting materials were processed as described above for sample 3. The T_g of such samples was found to be 254(2) °C (Fig. 3), the highest value of the four sets of samples synthesized in the present work.

Finally, we also prepared a crystalline $AgPO_3$ sample by heating sample 4 to 360 °C for 12 h, followed by cooling to room temperature over approximately 4 h. X-ray diffraction and Raman scattering experiments confirm the polymeric crystalline phase of the sample in both types of experiment.[17,22,37,38]

B. Modulated differential scanning calorimetry

A model 2920 modulated differential scanning calorimetry (MDSC) from TA Instruments Inc. was used to study glass transitions. In all experiments, we used a 3 °C/min scan rate and a 1 °C/100 s modulation rate. Typically 15–20 mg of a sample in platelet form was hermetically sealed in an Al pan and placed in the calorimeter head along with a reference pan. Details of the method have been discussed in earlier reports.[39,40] The component of total heat flow (Fig. 1) that tracks the sinusoidal temperature modulations is called *reversing* (Fig. 1). The difference between the total and reversing heat flow signals represents the *nonreversing* heat flow signal, and it usually displays a Gaussian-like peak [Fig. 1 (red)], as a precursor to the glass transition. The integrated area under the peak, henceforth defined as ΔH_{nr}, provides the nonreversing enthalpy of the glass transition. Furthermore, frequency-corrected ΔH_{nr} term was deduced in the usual way by integrating the heat going up and subtracting the corresponding heat coming down in temperature.[39] The inflection point of the reversing heat flow signal was used to define the glass transition temperature (T_g).

MDSC scans were performed on both as-quenched or virgin and T_g-cycled glass samples. The T_g-cycled samples were obtained by heating virgin samples in the calorimeter head to T_g. Figure 1 gives MDSC scans of sample 1 in its virgin (top panel) and T_g-cycled states (bottom panel). The results show a T_g of 181(2) °C for such a sample. Parallel results were obtained on sample 2, and the T_g was found to be 203 °C, about 20 °C higher than that of sample 1. Figure 2 gives MDSC scans of sample 3, in its virgin (top panel) and T_g-cycled states (middle panel) using $AgNO_3$ and $NH_4H_2PO_4$ as the precursors. The bottom panel of Fig. 2 shows a MDSC scan of a glass sample in a T_g-cycled state obtained using Ag_3PO_4 and P_2O_5 as precursors. Figure 3 gives MDSC scans of sample 4 in its virgin (top panel) and T_g-cycled states (bottom panel).

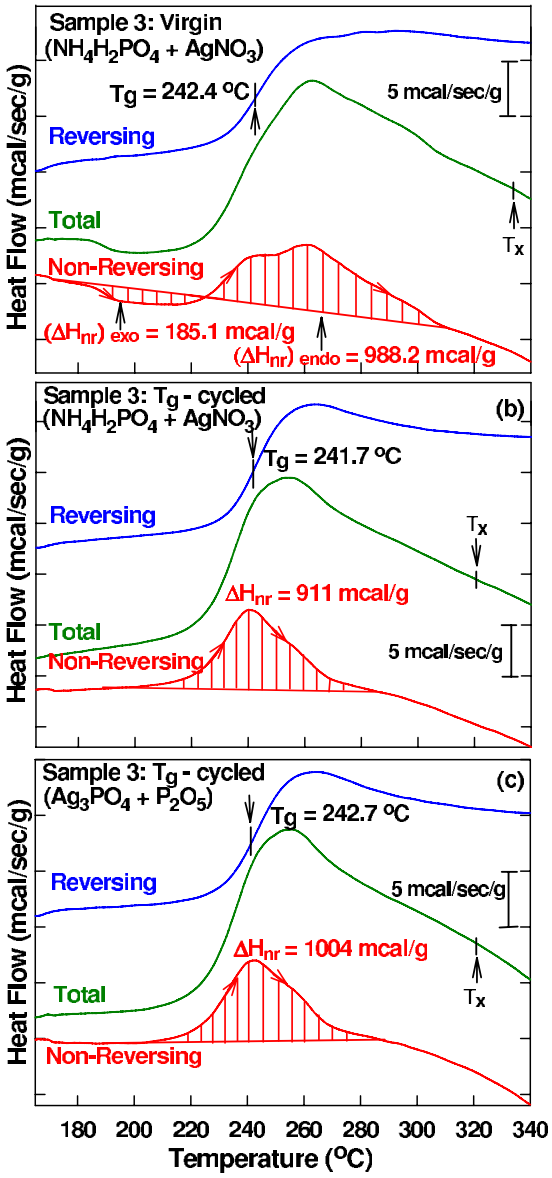

FIG. 2. (Color online) MDSC scan of sample 3 of $AgPO_3$ glass in its (a) virgin and (b) T_g-cycled state using $NH_4H_2PO_4$ and $AgNO_3$ as precursors. Upon T_g cycling, the glass transition narrows and the precursive exotherm present in the virgin samples disappears. (c) MDSC scan of sample 3 this time synthesized using Ag_3PO_4 and P_2O_5 as precursors. Note the similarity of results in (b) and (c). T_x represents the crystallization temperature.

Several features of the glass transition endotherm become transparent from the data of Figs. 1–3. In general, virgin samples show an exotherm before onset of the glass transition endotherm. Upon T_g cycling, the exotherm disappears and the glass transition endotherms become narrower and better defined. This observation corroborates previous findings by Tomasi *et al.*,[30] who observed exotherms in fast-quenched samples but not in slow-cooled ones. In Fig. 2, the T_g of sample 3, prepared using two different sets of precursors, is found to be the same. The identity of the T_g's of these two samples underscores that one has reached the same final product using two separate synthesis routes. The widths of

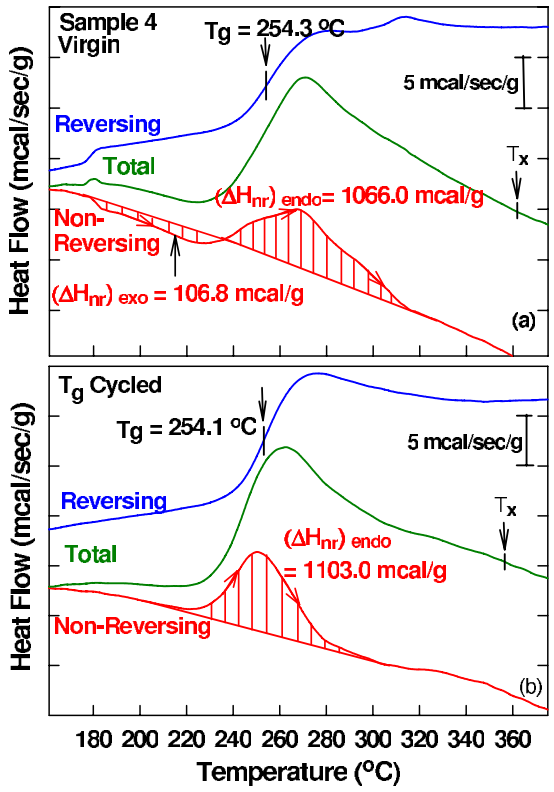

FIG. 3. (Color online) MDSC scan of sample 4 of $AgPO_3$ glass in its (a) virgin and (b) T_g-cycled state. Upon T_g cycling, the glass transition narrows and the precursive exotherm present in the virgin samples disappears. T_x represents the crystallization temperature.

the glass transitions as measured by those of the nonreversing heat flow peaks are found to be narrower for sample 1 (~20 °C), than for samples 3 and 4 (~40 °C). Finally, we find the T_g of sample 4 of 254(2) °C to be the highest of the four sets of samples synthesized in the present work. We shall return to discuss these results in the next section.

C. Raman scattering

A model T64000 triple-monochromator Raman-dispersive system from Horiba Jobin Yvon Inc., equipped with a charge-coupled device camera and a microscope (Olympus BX 41) was used to record Raman scattering. The scattering was excited with 514.1 nm radiation with a laser beam focused to a 2 μm spot size, using typically 1.2 mW of power incident on the sample. To avoid exposure to laboratory ambient (~50% RH), the measurements were performed with a sample mounted in an evacuated ($\sim 10^{-6}$ Torr) MMR Joule-Thompson refrigerator cold stage held at room temperature. The cold stage is a product of MMR Technologies, Mt. View, CA 94043. We extracted the mode frequency, width, and integrated intensity of the vibrational modes by least-squares fitting the observed line shapes to a superposition of Gaussian profiles with no restrictions on these three parameters.

We recorded Raman scattering from c-$AgPO_3$ [Fig. 4(c)]. The observed line shapes reveal sharp modes characteristic of a crystal. In sharp contrast, dry glass samples display [Fig. 4(b)] broad vibrational features, but with many of the features observed in the crystal. The Raman line shapes of samples 1 [Fig. 4(a)] and 4 [Fig. 4(b)] look superficially similar, but close examination reveals distinct differences. The background under the line shapes of sample 1 is found to be higher than for sample 4. This result most likely is due to increased structural disorder leading to residual scattering in the wet sample 1. Furthermore, the scattering strength ratio R of the P-O_t (1140 cm^{-1}) mode to the P-O_b mode (684 cm^{-1}) decreases as the sample T_g increases (Table I). Thus, for example, R=1.89 for the wet sample 1 with a T_g of

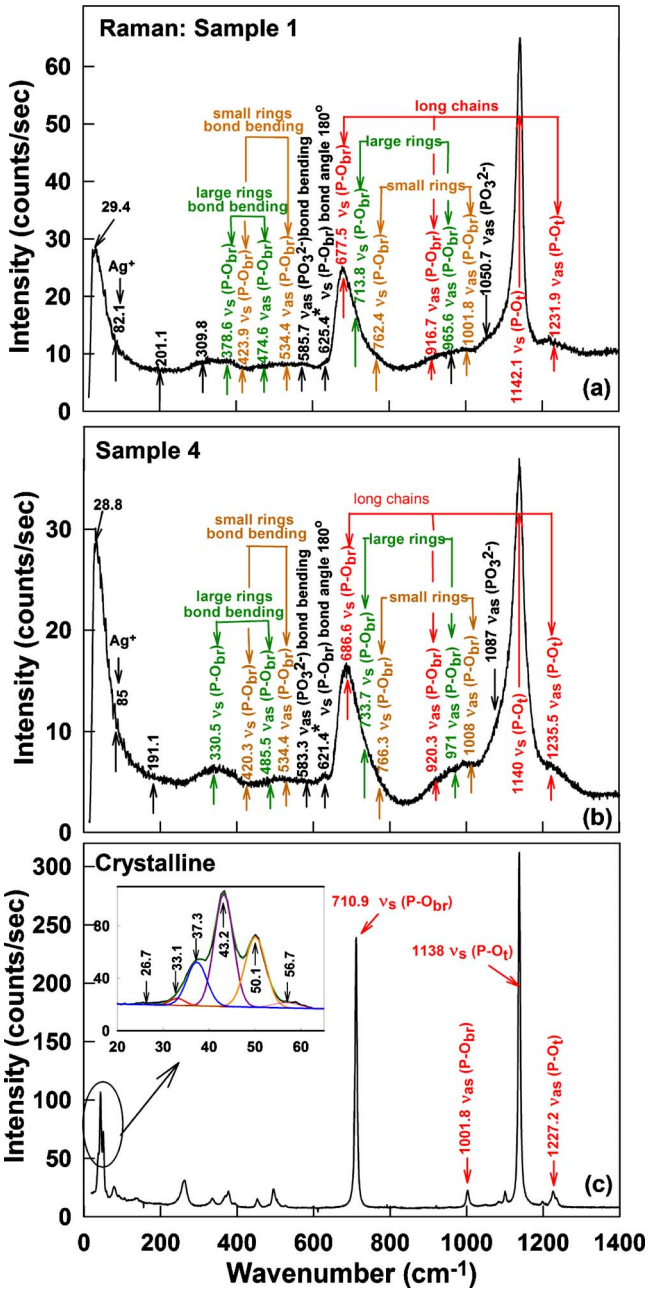

FIG. 4. (Color online) Raman scattering of $AgPO_3$ glass in (a) wet sample 1 and (b) dry sample 4. Residual scattering is higher in wet sample 1 than in dry sample 4, probably due to presence of greater structural disorder.

TABLE I. Glass transition temperature (T_g), integrated area ratio (R) of P-O_t and P-O_b modes, integrated intensity ratio of Boson peak to (P-O_t) mode, and molar volumes of *samples 1, 2, 3, and 4* synthesized in present work. N/A means not applicable.

Observable	g-$AgPO_3$ (*sample 1*)	g-$AgPO_3$ (*sample 2*)	g-$AgPO_3$ (*sample 3*)	g-$AgPO_3$ (*sample 4*)	c-$AgPO_3$
T_g (°C)	181(2)	203(2)	242(2)	254(2)	N/A
Long chains; $R=\frac{A_{\nu_s(\text{P-O}_t)}}{A_{\nu_s(\text{P-O}_{br})}}$	1.89	1.66	1.55	1.40	1.00
$\frac{I_{\text{Boson}}}{I_{\nu_s(\text{P-O}_t)}}$	0.45	0.68	0.89	0.95	N/A
Molar volume (cm^3/mol)	41.3(2)	41.7(2)	42.6(2)	44.2(2)	44.1(2)

181(2) °C, but it decreases to $R=1.40$ for the dry sample 4 with a T_g of 254(2) °C. The ratio $R=1$ in crystalline $AgPO_3$. These results are summarized in Table I. We shall discuss them in Sec. III.

D. Infrared reflectance

A Thermo-Nicolet FTIR research grade 900 Bench was used to record ir reflectance from glass samples. Typically glass samples were placed in a Seagull accessory, which provides for a variable angle of incidence of the ir beam, and reflectivity was recorded in both the mid-ir and far-ir ranges using an appropriate combination of detectors and beam splitters. We used a stainless steel mirror as a reference reflector to normalize the reflected light from the glass samples. We chose bulk samples with flat areas and gave no surface treatment prior to recording ir reflectance. A Kramers-Kronig transformation of the reflectance signal was performed to obtain absorption signals. The absorption results for both samples 1 and 4 in the far-ir and mid-ir regions appear in Fig. 5. Infrared absorption over a wider range appears in Fig. 6. An enlarged view of the boxed-in regions of Fig. 6 appears in Fig. 5.

There are three features of interest in Fig. 6. Above 1600 cm^{-1}, the ir absorbance in the wet sample 1 is higher than in the dry sample 4. The free water band[41,42] appears near 2807 cm^{-1}. It is a fairly broad band. The presence of the water band causes the baseline of the absorbance signal at frequencies exceeding 1600 cm^{-1} to be higher in sample 1 than in sample 4. Thus, there is more free water in sample 1 than in sample 4. The second feature relates to the absorbance of the sharp P-OH^- mode[41] around 2318 cm^{-1}, which is found to be ~0.3 in sample 1 but ~0.1 in sample 4, and for the mode around 2350 cm^{-1} to be ~0.35 in sample 1 but ~0.1 in sample 4 (see inset in Fig. 6). The absorbance of the sharp P-OH^- modes in the wet sample 1 exceeds that in the dry sample 4 by a factor of 3 or more. We take these results to show that there is more bonded water (OH) in the P-O-P chains in the wet sample 1 than in the dry sample 4, leading to splicing of the P-O-P chain network by dangling OH^- ends replacing bridging O sites.

The third feature relates to the absorbance signal in the 0–1200 cm^{-1} range (the red box in Fig. 5). The absorbance in the wet sample 1 exceeds that in the dry sample 4 by at least a factor of 4. This is a rather striking result. We will show later that the result highlights the very special role of free water vibrations coherently coupling with the Ag^+ ion floppy modes in enhancing the ir response of optic modes of the P-O-P chains and rings. To facilitate a direct comparison, we provide in Fig. 7 the published results of Kamitsos *et al.*[43] along with the present results for the wet sample 1 and the dry sample 4. In Fig. 7, the low-frequency ir response of our samples was recorded using a Si bolometer detector. In both the wet and dry samples we can observe the floppy modes associated with the Ag^+ cation motion near 44.1 and 139.7 cm^{-1}. Finally, we note that the ir response of our wet sample 1 is remarkably similar to the results reported by Kamitsos *et al.*[43] These results suggest that previous work on $AgPO_3$ glass and on $AgPO_3$-AgI solid electrolyte glasses has most likely been on samples that are wet.

E. Mass density of glass samples

The mass density of the glass samples was measured using the Archimedes principle. We used a quartz fiber with hooks at both ends, permitting it to be suspended from a pan of an electronic balance, to measure the mass of a glass sample suspended in air or in pure alcohol. The density of alcohol was calibrated using a Si single crystal. For a glass sample of 100 mg or more, one could obtain the mass density to an accuracy of about 1% or less using this arrangement. The mass density was used to calculate the molar volumes of the glass samples, which are summarized in Table I. For sample 1, the molar volumes are almost identical to the ones reported by two other groups,[15,44] but the molar volume of our dry sample 4 is found to be larger than that of the wet sample 1.

III. DISCUSSION

A. Molecular structure of $AgPO_3$ glass

The Raman line shapes of crystalline and glassy $AgPO_3$ share commonalities; in both instances the vibrational density of states is dominated by two modes, the symmetric vibration of P-O_t near 1140 cm^{-1} and that of P-O_b near 680 cm^{-1}. These results have led to the general recognition

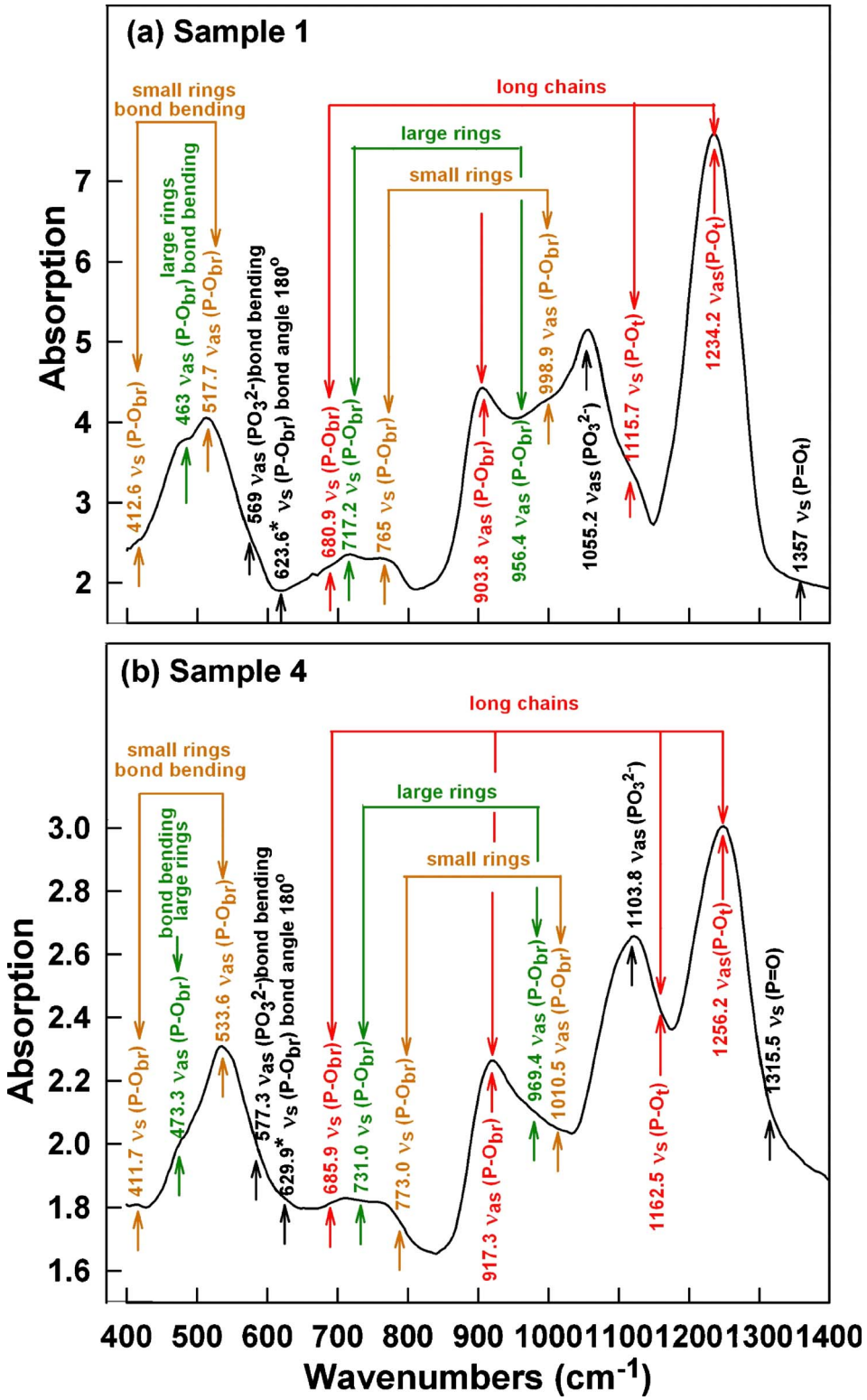

FIG. 5. (Color online) Infrared absorption of $AgPO_3$ glass in (a) wet sample 1 and (b) dry sample 4. The absorption signals in the far- and mid-ir range are much higher in sample 1 than in 4. High frequency response in mid-ir range in the samples is presented in Fig. 6.

that the glass, in analogy to the crystal, consists largely of polymeric chains of PO_4 units having two bridging and two terminal atoms, or Q^2 units in the NMR notation. There are other vibrational features observed in the glass that are much weaker in scattering strength, which can be attributed to the presence of Q^2 species present in rings of both large and small (Fig. 5) size. The mode assignments are facilitated by previous work in the field.[43,45,46] In addition, at low frequencies, one observes the Boson mode[29] near 29 cm^{-1}, a feature peculiar to the glass phase.

Some confidence in vibrational mode assignments is afforded by the ir results, which reveal the asymmetric counterparts of the symmetric vibrations seen in Raman scattering. Specifically, the asymmetric vibrations of the P-O_t

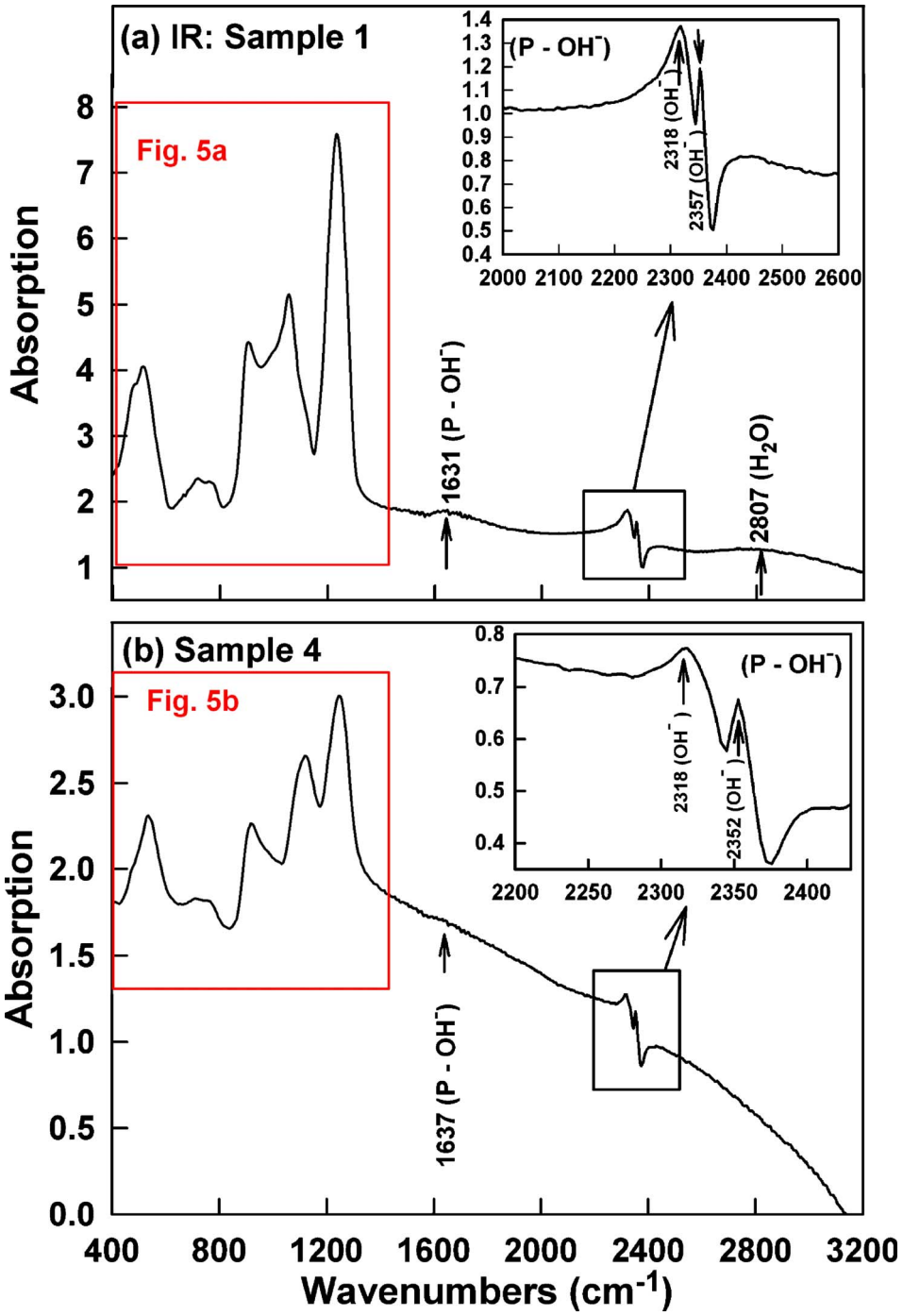

FIG. 6. (Color online) ir absorption of $AgPO_3$ glass in (a) sample 1 and (b) sample 4 showing features in the high frequency of mid-ir. A blowup of the mid-ir region consisting of the two main modes of PO_4 tetrahedra is shown separately in Fig. 5. Water bands and vibrational modes associated with P-OH^- species are readily observed in sample 1, but are much weaker in sample 4. Note that the absorption scale has been enlarged in (b) to permit viewing the sharp feature in question.

bonds around 1230 cm^{-1} and of P-O_b bonds around 900 cm^{-1} in long chains, and likewise the asymmetric vibrations of Q^2 units present in small rings and large rings are strongly excited in the ir as shown in Fig. 5. The broad picture suggested is that the glassy phase largely consists of polymeric chains with small fraction of rings. In addition to these structural groupings, the glassy phase also consists of terminal $(PO_3)^{2-}$ units or Q^1 species that terminate chains. The vibrational feature around 1050 cm^{-1} in Raman and 1055 cm^{-1} in ir spectra is associated with these Q^1 species. ^{31}P and ^1H NMR experiments on the present glass samples are currently on going and will be reported in future.[47] We shall then reconsider the results of Fig. 6 in connection with water codoping in the $AgPO_3$ glass.

A ubiquitous feature of Raman scattering results on $AgPO_3$ glasses is the presence of the low-frequency mode near 29 cm^{-1} identified as the Boson peak.[29] The scattering strength of this mode appears to increase steadily in the sequence sample $1 \rightarrow 2 \rightarrow 3 \rightarrow 4$ as the T_g's increase and the samples get drier (Table I). For example, in sample 1, the Boson peak is nearly half as high in intensity as the P-O_t mode, but in sample 4, the Boson peak intensity nearly equals that of the P-O_t mode. Although the nature of the Boson peak continues to be a subject of ongoing

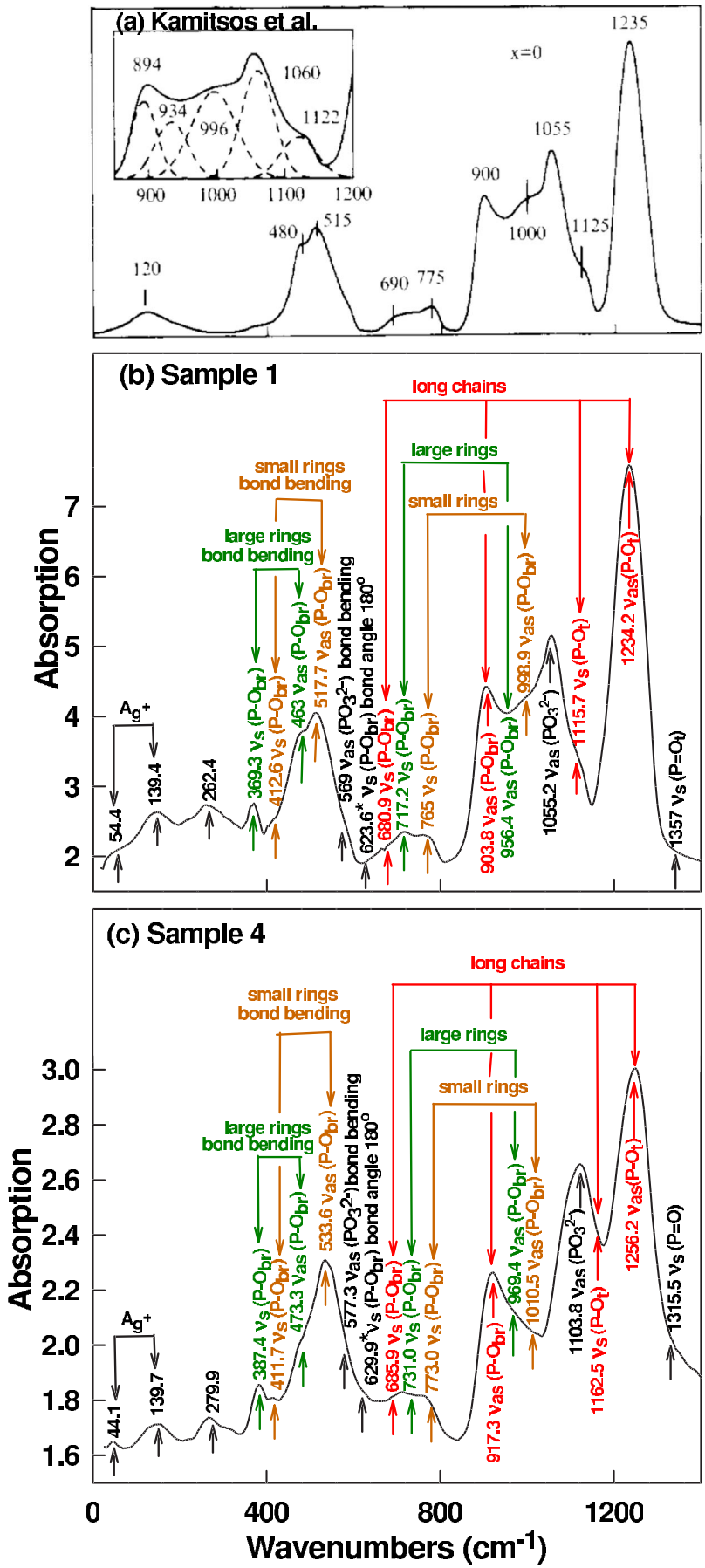

FIG. 7. (Color online) Infrared absorption of $AgPO_3$ glass (a) reported by Kamitsos *et al.* (Ref. 43), (b) observed in present work on wet sample 1, and (c) observed in present work on dry sample 4. In (b) and (c) a Si bolometer detector was used to record the response at low frequencies (<400 cm^{-1}).

discussions,[48–51] the most natural interpretation of these data is that the intermediate-range order of $AgPO_3$ glass samples becomes better defined as the T_g increases to 254(2) °C (sample 4). That view is independently corroborated by the background underneath the Raman modes, which is lower in sample 4 than in sample 1. Some structural-disorder-induced residual scattering appears in sample 1, but that scattering is nearly absent in sample 4. In these experiments, the structural disorder results from cutting of the P-O-P chain network due to the presence of bonded water as discussed in Sec. III C.

B. Frozen-in strain in freshly quenched $AgPO_3$ glass

Freshly quenched $AgPO_3$ glasses are highly strained. The evidence comes from exotherms observed in virgin samples at temperatures below T_g, for example, near $T=160$ °C in sample 1 (Fig. 1), near $T=200$ °C in sample 3 (Fig. 2), and near $T=210$ °C in sample 4 (Fig. 3). By heating a virgin glass sample close to T_g, one dissipates the frozen-in strain as the chain network thermally relaxes. These results bearing on the structural relaxation of virgin glasses close to T_g are in harmony with the results of Mustarelli *et al.*[30] In Ref. 30, the authors also observed evidence of an exotherm in fast-quenched samples but not in slow-cooled ones. Modulated DSC scans of glass transition endotherms (Figs. 1–3) in virgin samples show the nonreversing heat flow signals to be rather broad in temperature, but upon thermally cycling samples through T_g, these become narrower. These data suggest that virgin samples consist of a network of broken chains, which upon heating close to T_g polymerize into longer chains. In the T_g-cycled samples, the narrow width of the glass transition for sample 1 of about 20 °C is characteristic[51] of elastically flexible glasses, while the broad (~30 °C) and asymmetric profile of the glass transition of sample 4 is characteristic of a stressed rigid glass network.[51] In our studies of the percolation of rigidity in chalcogenide glasses,[6,51] we have found weakly cross-linked networks to be in the flexible phase while heavily cross-linked networks are in a stressed-rigid phase. Counting of mechanical constraints in oxide glasses is less obvious because the coordination numbers of cations and anions are not always clear. But these trends in the widths of the glass transition endotherm strongly reinforce the idea that sample 4 possesses a network of higher connectivity than sample 1; and the reduction of T_g upon water doping of sample 4 leads in a natural way to a loss in connectedness of the glass structure.

C. Water doping, glass structure, and magnitude of T_g

Perhaps the most striking result of the present work is the wide variation in glass transition temperatures due to sample processing. The T_g value of 254(2) °C for sample 4 is by far the highest value reported to date for an $AgPO_3$ glass (Fig. 7). The T_g value of sample 1 is typical (Fig. 7) of previous reports.[15,26–31] T_g provides a good measure of network connectivity as elucidated by the work of Micoulaut and Kerner.[52] Recently, Naumis *et al.*[53] has independently shown that chemical trends in T_g scale well with Lindemann's melting criteria and the rigidity of a network as gauged by the Lamb-Mössbauer mean-square displacements.[54,55] Thus, the higher T_g of dry $AgPO_3$ samples suggests that the network connectivity of such samples must be higher. That view is independently corroborated by the nature of the nonreversing enthalpy of T_g as mentioned earlier. For wet $AgPO_3$ samples, one finds ΔH_{nr} profiles to be narrow (~20 °C wide) and symmetric in temperature [Fig. 1(b)], features associated with flexible glasses. On the other hand, for dry samples, ΔH_{nr} profiles are wide (40 °C wide) and asymmetric with a high-T tail [Fig. 3(b)], which are characteristic of stressed-rigid glasses.

The behavior observed here is reminiscent of the sharp reduction of T_g of a SiO_2 or GeO_2 glass when alloyed with a few mole percent of soda. A parallel behavior is noted with water as an additive in silicate melts.[56] The stoichiometric $AgPO_3$ glass structure is better visualized as a 3D connected chain structure with Ag^+ ions serving as the cross-links between chains rather than as composed of isolated 1D chains of PO_4 tetrahedra.

Mustarelli *et al.*[26] have synthesized glass samples by fusing stoichiometric amounts of $AgNO_3$ with $NH_4H_2PO_4$ in air using Pt crucibles, and have annealed melts at temperatures in the $500<T_a<700$ °C range for varying time periods in the range $10<t<360$ min. Here, T_a represents the annealing temperature of the melts. The melts were then poured between Al blocks at room temperature to realize bulk glasses. The T_g's of the samples were found to steadily increase in the $165<T_g<186.7$ °C range, as T_a increased in the $500<T_a<700$ °C range. The highest T_g of 189.2 °C was realized by melting crystalline $AgPO_3$. We have projected the highest T_g obtained by Mustarelli *et al.*[26] in the plot of Fig. 8.

The T_g's reported by Mustarelli *et al.*[26] are quite similar to those reported by several groups, including us, when the starting materials are handled in *air*, as can be seen in Fig. 8. These values are significantly lower than the value we obtained for our sample 4 when precursors were handled in a dry ambient environment. These data suggest that once water is bonded in a $AgPO_3$ glass, it is difficult to remove it by thermally annealing melts at 700 °C for extended periods. Comprehensive ^{31}P and ^{1}H NMR experiments on our samples are currently in progress.[47] A comparison of these results with those of Mustarelli *et al.*[26] should permit elucidation of the role of water in the structure and glass transition temperature.

The presence of free water in $AgPO_3$ has some profound consequences for the ir response (Sec. II D) of glasses, a recognition that emerged only when results on the dry sample 4 could be compared with those on the wet sample 1 in the present work (Figs. 5 and 7). The molecular structure of the glass allows for Ag^+ ions to dress the edges of the network of P-O-P chains and rings. In such a structure, free water resides in between the chains and rings, and in proximity to the Ag^+ ions. The collective modes of water can lock onto the Ag^+ floppy modes (50 and 140 cm^{-1}), and lead to a long-range coherent enhancement of oscillator strength of all the optic modes associated with the P-O-P chains and rings (modes observed in the 400–1200 cm^{-1} range). When the water content of the glasses decreases, as for example in the dry sample 4, the icelike films on the chains must break

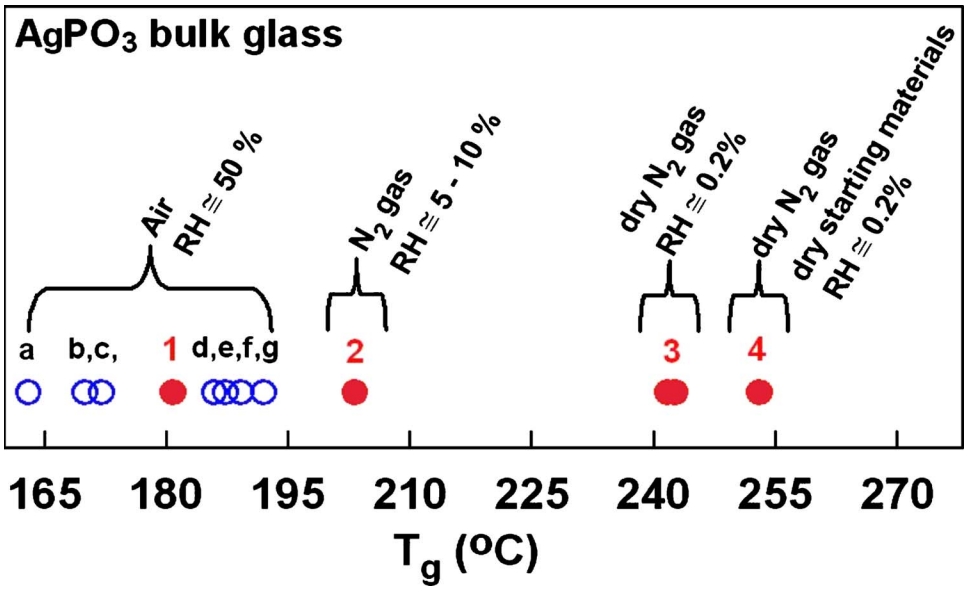

FIG. 8. (Color online) T_g of $AgPO_3$ glass samples reported in the literature (○) compared to those obtained in present work (red filled circle). The literature values are characteristic of samples processed at laboratory ambient (a) T_g=163 °C (Ref. 28); (b) T_g=170 °C (Ref. 29); (c) T_g=172 °C (Ref. 15); (d) T_g=185.9 °C (Ref. 27); (e) T_g=187.3 °C (Ref. 30); (f) T_g=189.2 °C (Ref. 26); (g) T_g=192 °C (Ref. 31). The red solid circles are results of our measurements. See text for details.

up into patches and become incoherently pinned, leading to a dramatic loss of ir response [compare Figs. 7(b) and 7(c)]. The fourfold enhancement of the ir response of optic modes associated with P-O-P chains and rings in wet glass samples in relation to the dry ones most likely has such an origin. Fourier-transform ir has served as a powerful research tool to elucidate the physical behavior and structure of carbohydrates. Water in carbohydrates also enhances ir activity, and the correlation between structure and ir activity enhancement is a subject of current interest in cell dynamics.[57]

Raman scattering (Table I) has also proved quite diagnostic in elucidating the presence of water in $AgPO_3$ glass samples. We find that the scattering strength ratio R of P-O_t (around 1140 cm^{-1}) to P-O_b (around 680 cm^{-1}) vibrations in chains is near unity in c-$AgPO_3$ [Fig. 4(c)]. If the Raman cross sections of the two modes in question were identical, the result would imply that, for infinitely long chains, one has equal numbers of bridging and terminal oxygen neighbors in the crystalline phase. Furthermore, the ratio R increases to 1.40 in sample 4 and to 1.89 in sample 1. The simplest interpretation is that absorption of water depolymerizes the -P-O-P chains by transforming two Q^2 species into two Q^1 species. A terminal OH^- anion couples to one end of a chain while the H^+ links with the dangling O^{2-} to create a terminal OH^- on the other. Our ir measurements reveal two closely spaced vibrations around 2318 and 2350 cm^{-1} (Fig. 6) that we associate with the OH^- stretch of the terminal P-OH^-. The reaction of water is to systematically convert some of the P-O_b bonds into P-OH^- bonds and reduce the length of the P-O-P chains. Consequently, upon water codoping, one expects the ratio R to increase as the count of P-O_t bonds remains unchanged but that of P-O_b bonds systematically decreases. The concentration of the P-OH^- bonds in sample 4 [Fig. 6(b)] must be lower than in sample 1 [Fig. 6(a)], but to deduce the concentrations of these species a knowledge of the Raman cross sections becomes necessary.

D. Network packing and water content of glasses

The molar volume of $AgPO_3$ glass (Table I) systematically decreases in the $4 \rightarrow 1$ sequence. The result suggests that the presence of codoped water (H^+ and OH^-) in the glasses leads to fragmentation of the metaphosphate P-O-P chain network, leading to better packing. The result lowers not only the glass transition temperature (Fig. 8) but also the molar volume (Table I). The molar volume of sample 1 [41.3(2) cm^3/mol] is similar to the value reported by Sidebottom[15] (41.71 cm^3/mol) and by Lee and Elliott[44] (41.52 cm^3/mol). On the other hand, the molar volume of sample 4 (44.20 cm^3/mol) nearly equals that of c-$AgPO_3$ (Table I).

IV. CONCLUDING REMARKS

We have synthesized four sets of $AgPO_3$ glass samples (samples 1–4) by mixing the usual precursors in steadily drier ambient environments. Sample 1 was prepared by handling the precursors at laboratory ambient (relative humidity ~50%) while sample 4 was prepared by handling the precursors in a high-purity dry-N_2-gas-purged glove box with a relative humidity of less than 0.2%. The glass transition temperatures of the samples steadily increase in the sequence $1 \rightarrow 4$, with sample 1 possessing a T_g of 181(2) °C, characteristic of a wet sample, while sample 4 possesses a T_g of 254(2) °C characteristic of a dry sample. The ir reflectance reveals modes of both free and bonded water in the samples, with the concentration of these species decreasing qualitatively in the sequence $1 \rightarrow 4$. The special role of water in $AgPO_3$ glass in enhancing the ir response of the optic modes appears to be a general feature that is observed in other network glasses as well as molecular glasses such as carbohydrates[10,11,13] and probably proteins.[57] Raman scattering reveals that the scattering strength ratio R of P-O_t (terminal) to P-O_b (bridging) decreases steadily (Table I) in the sequence $1 \rightarrow 4$, an observation that is consistent with the P-O-P chains being steadily broken as OH^- terminal bonds (from water) replace bridging O. The Boson peak scattering strength steadily increases in the sequence $1 \rightarrow 4$ (Table I), suggesting that intermediate-range order of glasses becomes best defined in the driest sample 4. The molar volumes of the

samples increase steadily in the sequence $1 \rightarrow 4$, with sample 4 possessing a molar volume nearly the same (Table I) as that of c-$AgPO_3$. The broad picture suggested by these results is that the stoichiometric glass largely consists of a 3D network of interconnected zigzag chains of PO_4 tetrahedra with a finite concentration of Q^1 species. Sample 4, the driest of the sets investigated, possesses the least amount of codoped water, the highest T_g, the largest molar volume, and the best defined intermediate range-order as determined by the integrated intensity of the boson peak.

We have recently examined[19] the physical properties including electrical conductivity and structural evolution of dry solid electrolyte glasses of the composition $(AgPO_3)_{1-x}(AgI)_x$ as a function of AgI content. Results on these dry samples provide evidence[19] of two sharply defined compositional thresholds in the electrical conductivity near $x=9.5\%$ and 37.8%, which represent, respectively, the *stress* and *rigidity* elastic phase boundaries in these solid electrolyte glasses. These compositional trends in conductivity of dry samples differ significantly from previous reports[15,17,18,24,58–60] on the same glass system, and it is possible that these differences in behavior are related to the presence of water in samples.

ACKNOWLEDGMENTS

We have benefited from several insights provided by J. C. Phillips during the course of this work. This work was supported by U.S. NSF Grants No. DMR 04 -56472 and No. IMR-03-15491.

[1] V. N. Naraev, Glass Phys. Chem. **30**, 367 (2004).
[2] M. Takata, M. Tomozawa, and E. B. Watson, J. Am. Ceram. Soc. **65**, 91 (1982).
[3] V. Rompicharla, T. Qu, S. Mamedov, P. Boolchand, M. Micoulaut, and Y. Vaills, Bull. Am. Phys. Soc. **49**, 613 (2004).
[4] V. Rompicharla, S. Mamedov, P. Boolchand, A. Basu, and M. Micoulaut, in *Abstracts of the Ninth International Conference on the Structure of Non-Crystalline Materials*, Corning, NY, July 11-15, 2004 (unpublished).
[5] P. Boolchand, http://www.ececs.uc. edu/~pboolcha/interest.htm
[6] F. Wang, S. Mamedov, P. Boolchand, B. Goodman, and M. Chandrasekhar, Phys. Rev. B **71**, 174201 (2005).
[7] P. Boolchand, M. Zhang, and B. Goodman, Phys. Rev. B **53**, 11488 (1996).
[8] F. Wang, P. Boolchand, K. A. Jackson, and M. Micoulaut, J. Phys.: Condens. Matter **19**, 226201 (2007).
[9] B. Mysen and P. Richet, *Silicate Glasses and Melts: Properties and Structure* (Elsevier, Amsterdam, 2005).
[10] M. Kacurakova and M. Mathlouthi, Carbohydr. Res. **284**, 145 (1996).
[11] M. Kacurakova and R. H. Wilson, Carbohydr. Polym. **44**, 291 (2001).
[12] K. Akao, Y. Okubo, T. Ikeda, Y. Inoue, and M. Sakurai, Chem. Lett. **1998**, 759.
[13] G. Caliskan, D. Mechtani, J. H. Roh, A. Kisliuk, A. P. Sokolov, S. Azzam, M. T. Cicerone, S. Lin-Gibson, and I. Pearl, J. Chem. Phys. **121**, 1978 (2004).
[14] R. K. Brow, J. Non-Cryst. Solids **263**, 1 (2000).
[15] D. L. Sidebottom, Phys. Rev. B **61**, 14507 (2000).
[16] C. Holbrook, P. Chen, P. Boolchand, and D. I. Novita, IEEE Trans. Nanotechnol. **6**, 530 (2007).
[17] J. D. Wicks, L. Borjesson, G. Bushnell-Wye, W. S. Howells, and R. L. McGreevy, Phys. Rev. Lett. **74**, 726 (1995).
[18] M. Mangion and G. P. Johari, Phys. Rev. B **36**, 8845 (1987).
[19] D. I. Novita, P. Boolchand, M. Malki, and M. Micoulaut, Phys. Rev. Lett. **98**, 195501 (2007).
[20] C. Angell, Annu. Rev. Phys. Chem. **43**, 693 (1992).
[21] M. Shizukuishi *et al.*, Jpn. J. Appl. Phys. **20**, 581 (1981).
[22] V. K. H. Jost, Acta Crystallogr. **14**, 779 (1961).
[23] Y. S. Bobovich, Opt. Spektrosk. **13**, 492 (1962).
[24] S. W. Martin, J. Am. Ceram. Soc. **74**, 1767 (1991).
[25] Y. Abe, in *Topics in Phosphorus Chemistry*, edited by M. Grayson and E. J. Griffith (Wiley, New York, 1983), Vol. 11, p. 19.
[26] P. Mustarelli, C. Tomasi, A. Magistris, and S. Scotti, J. Non-Cryst. Solids **163**, 97 (1993).
[27] A. Schiraldi, E. Pezzati, and P. Baldini, Phys. Chem. Glasses **27**, 190 (1986).
[28] E. Kartini, M. F. Collins, T. Priyanto, M. Yusuf, N. Indayaningsih, E. C. Svensson, and S. J. Kennedy, Phys. Rev. B **61**, 1036 (2000).
[29] F. Rossi, A. Fontana, and L. Righetti, Philos. Mag. B **82**, 323 (2002).
[30] C. Tomasi, P. Mustarelli, and A. Magistris, Phys. Chem. Glasses **36**, 136 (1995).
[31] A. Hallbrucker and G. P. Johari, Phys. Chem. Glasses **30**, 211 (1989).
[32] P. Boolchand, G. Lucovsky, J. C. Phillips, and M. F. Thorpe, Philos. Mag. **85**, 3823 (2005).
[33] P. Boolchand, D. G. Georgiev, and B. Goodman, J. Optoelectron. Adv. Mater. **3**, 703 (2001).
[34] M. Micoulaut and J. C. Phillips, Phys. Rev. B **67**, 104204 (2003).
[35] M. F. Thorpe, D. J. Jacobs, M. V. Chubynsky, and J. C. Phillips, J. Non-Cryst. Solids **266**, 859 (2000).
[36] Y. Wang, J. Wells, D. G. Georgiev, P. Boolchand, K. Jackson, and M. Micoulaut, Phys. Rev. Lett. **87**, 185503 (2001).
[37] A. Rulmont, R. Cahay, M. Liegeois-Duyckaerts, and P. Tarte, Eur. J. Solid State Inorg. Chem. **28**, 207 (1991).
[38] I. Belharouak, E. Fargin, C. Parent, G. Le Flem, H. Aouad, M. Mesnaoui, and M. Maazaz, Solid State Sci. **1**, 287 (1999).
[39] Leonard C. Thomas, Modulated DSC Technology, T. A. Instruments Inc., 2007, www.TAInstruments.com
[40] T. Qu and P. Boolchand, Philos. Mag. **85**, 875 (2005).
[41] A. M. Efimov and V. G. Pogareva, J. Non-Cryst. Solids **275**, 189 (2000).
[42] N. B. Colthup, L. H. Daly, and S. E. Wiberley, in *Introduction to Infrared and Raman Spectroscopy* (Harcourt Brace & Company, San Diego, CA, 1990), p. 365.
[43] E. I. Kamitsos, J. A. Kapoutsis, G. D. Chryssikos, J. M. Hutchinson, A. J. Pappin, M. D. Ingram, and J. A. Duffy, Phys. Chem. Glasses **36**, 141 (1995).

[44] J. H. Lee and S. R. Elliott, Phys. Rev. B **54**, 12109 (1996).
[45] J. P. Malugani and R. Mercier, Solid State Ionics **13**, 293 (1984).
[46] M. C. R. Shastry and K. J. Rao, Spectrochim. Acta, Part A **46**, 1581 (1990).
[47] F. Fayon, D. Massiot, K. Suzuya, and D. L. Price, J. Non-Cryst. Solids **283**, 88 (2001).
[48] M. I. Klinger and A. M. Kosevich, Phys. Lett. A **280**, 365 (2001).
[49] C. A. Angell, J. Phys.: Condens. Matter **16**, S5153 (2004).
[50] T. S. Grigera, V. Martin-Mayor, G. Parisi, and P. Verrocchio, Nature (London) **422**, 289 (2003).
[51] P. Boolchand, X. Feng, and W. J. Bresser, J. Non-Cryst. Solids **293**, 348 (2001).
[52] R. Kerner and M. Micoulaut, J. Non-Cryst. Solids **210**, 298 (1997).
[53] G. Naumis, Phys. Rev. B **73**, 172202 (2006).
[54] P. Boolchand, R. N. Enzweiler, R. L. Cappelletti, W. A. Kamitakahara, Y. Cai, and M. F. Thorpe, Solid State Ionics **39**, 81 (1990).
[55] P. Boolchand, W. Bresser, M. Zhang, Y. Wu, J. Wells, and R. N. Enzweiler, J. Non-Cryst. Solids **182**, 143 (1995).
[56] J. Deubener, R. Muller, H. Behrens, and G. Heide, J. Non-Cryst. Solids **330**, 268 (2003).
[57] J. C. Phillips Phys. Rev. B **73**, 024210 (2006)
[58] M. Lestanguennec and S. R. Elliott, Solid State Ionics **73**, 199 (1994).
[59] S. Bhattacharya, D. Dutta, and A. Ghosh, Phys. Rev. B **73**, 104201 (2006).
[60] C. Tomasi, P. Mustarelli, A. Magistris, and M. P. I. Garcia, J. Non-Cryst. Solids **293**, 785 (2001).